Creating Isogenic Cell Cultures for Functional Studies

of DNA Mismatch-Repair

By Kimberly Sarver

A PROJECT

Submitted to

Oregon State University

In partial fulfillment of

the requirements for the

degree of

Baccalaureate of Science in Bioresource Research

Presented: April 30, 2015

Commencement June 2015

AN ABSTRACT OF THE THESIS OF

<u>Kimberly A. Sarver</u> for the degree of Baccalaureate of Science in Bioresource Research presented on April 30th, 2015. Title: Creating Isogenic Cell Cultures for Functional Studies of DNA Mismatch-Repair

Abstract approved:

_____

Andrew Buermeyer

Colorectal cancer (CRC), the third leading cause of cancer death in the USA, depends on early detection for patient survival. Early detection is improved with the identification of high risk individuals. Risk of CRC development is a complex interaction between an individual's genetics and environmental exposures. Polycyclic Aromatic Hydrocarbons (PAHs) are ubiquitous, priority pollutants formed from the incomplete combustion of carbon. 96% of PAH exposure is through the diet for non-smokers. Metabolism of PAHs can form diol epoxides capable of binding to DNA, causing bulky DNA adducts which can lead to mutations and cancer. Preliminary data suggest that DNA mismatch repair (MMR) modulates mutagenicity of PAHs. Successful MMR depends on the formation of the MutSα protein complex, a heterodimer of MSH2 and MSH6 proteins. The objective of this project was to create a model system with which to perform functional assays for MMR capacity. I hypothesized that transfecting MMR-proficient cells with siRNA (short interfering RNA) would be a useful approach for creating isogenic cell cultures with MMR deficiencies without preexisting mutations or high spontaneous mutation rates. A MMR-proficient cell line, HeLa, was transfected with siRNA specific for the *MLH1* and *MSH2* genes. Analysis of anti-MLH1 and anti-MSH2 transfected cultures through semi-quantitative immunoblotting demonstrated a reduction in protein accumulation of MLH1, MSH2 and MSH6 respectively between 48 and 72 hours post-transfection, relative to the

untransfected and negative-control-transfected cells. To determine the effect of reduced MSH2 protein accumulation on the MMR capacity of cells post-transfection I measured the survival of cells after exposure to the purine analog 6-Thioguanine (6-TG). Cells transfected with anti-MSH2 siRNA did not respond as expected and demonstrated no significant difference in survival between the anti-MSH2 transfected cultures and cultures transfected with Allstars Negative control siRNA or the untransfected cultures.

Key Words: DNA Mismatch Repair, Polycyclic Aromatic Hydrocarbons, Cancer, siRNA

Corresponding Email Address: SarverK@oregonstate.edu

Creating Isogenic Cell Cultures for Functional Studies

of DNA Mismatch-Repair

By Kimberly Sarver

A PROJECT

Submitted to

Oregon State University

In partial fulfillment of

the requirements for the

degree of

Baccalaureate of Science in Bioresource Research

Presented: April 30, 2015

Commencement June 2015

Baccalaureate of Science in Bioresource Research project of Kimberly Sarver

Presented on April 30, 2015

APPROVED:

_____

Dr. Andrew B. Buermeyer, representing Environmental and Molecular Toxicology

_____

Dr. Dave Stone, representing Environmental and Molecular Toxicology

_____

Dr. Katharine Field, Department of Bioresource Research

I understand that my project will become part of the permanent collection of Oregon State University. My signature below authorizes release of my project to any reader upon request.

_____

Kimberly Sarver, Author

Acknowledgements

Table of Contents

List of Figures

List of Tables

List of Abbreviations

6-TG	6-Thioguanine
ACP	Adenomatous Polyposis Coli
ATCC	American Type Culture Collection
B[a]P	Benzo[a]pyrene
BCA	Bicinchoninic Acid
CRC	Colorectal Cancer
DMEM	Dulbecco's Modified Eagle's Medium
dsRNA	Double Stranded RNA
EGFR	Epidermal Growth Factor Receptor
EPA	Environmental Protection Agency
EXO 1	Exonuclease 1
FAP	Familial Adenomatous Polyposis
FBS	Fetal Bovine Serum
GST	Glutathione Transferase
HNPCC	Hereditary Non-Polyposis Colorectal Cancer (Lynch Syndrome)
HRP	Horseradish-Peroxidase-Conjugated
IDL	Inserion-Deletion Loops
MMR	Mismatch Repair
MOPS	N-Morpholino-Propane-Sulfonic Acid
mRNA	Messenger RNA
PAH	Polycyclic Aromatic Hydrocarbons
PCNA	Proliferating Cell Nuclear Antigen
PPB	Parts Per Billion

PPM	Parts Per Million
PVDF	Polyvinylidene Fluoride
RII	Tumor Growth Factor β Receptor
RISC	RNA-Induced Silencing Complex
RPA	Replication Protein A
siRNA	Short-Interfering RNA
TBST	Tris-Buffered Saline and Tween
UDP	Uridine Diphosphate
VEGF	Vascular Endothelial Growth Factor

Introduction

Colorectal Cancer

In 2014 the American Cancer Society estimated that colorectal cancer (CRC) was the third most commonly diagnosed cancer and the third leading cause of cancer death in the USA. Approximately 136,000 new cases and over 50,000 fatalities occurred in the US during 2014. 1 in 20 Americans will be diagnosed with colorectal cancer in their lifetime. CRC develops from pre-cancerous growths, called polyps, associated with DNA changes in cells within the lining of the colon. The most common types of polyps are known as adenomatous polyps or adenomas; these arise from glandular cells that secrete mucus to lubricate the colorectum. Adenomas are common in individuals over the age of 40. Approximately 10% of adenomas can become a malignant cancer called an adenocarcinoma over the course of 5-10 years if left untreated. The likelihood of an adenoma evolving into cancer increases as the adenoma increases in size. Approximately 96% of colorectal cancers are adenocarcinomas. Colorectal cancer patients are often treated with chemotherapy after the removal of cancerous growths through surgery. Other targeted therapies include epidermal growth factor receptor (EGFR) inhibitors and vascular endothelial growth factor (VEGF) inhibitors. EGFR inhibitors often slow or stop cancer cell growth while VEGF inhibitors prevent the formation of new blood vessels necessary for tumor growth (Siegel and Jemal 2014).

Both the cancer incidence and death rates have declined significantly in the US during the past decade due to prevention as a result of early detection and removal of polyps through screening methods (Siegel and Jemal 2014). A colonoscopy, the most common screening technique, allows for a direct visual examination of the colon, and removal of any polyps

discovered during the process. At present, screening is only recommended for people aged 50

and older. Of those, only 59% reported having testing consistent with current guidelines in 2010.

High risk individuals, such as those with genetic predispositions to colorectal cancer

development, can develop adenomous polyps much earlier than age 50 (Siegel and Jemal 2014).

Thus, early identification of high-risk individuals and their families is important for

implementation of preventative measures and timely screening.

Despite improved preventative screening measures and the decline of CRC rates in the

US, the worldwide CRC incidence rate is on the rise, especially in developing countries.

Increased industrialization and adoption of a "western" diet rich in fat and meat are suggested to

be contributing to the rise in CRC rates (Bishehsari 2014). Data from López-Abente et al.

suggest that living or working in close proximity to industries with pollutant emissions to air

increases the CRC incidence rate among both men and women (López-Abente et al. 2012).

Environmental Factors in CRC

PAH Exposure

Polycyclic aromatic hydrocarbons (PAHs) are ubiquitous pollutants in the environment

and are classified as priority pollutants by the U.S. Environmental Protection Agency (EPA).

Many distinct PAHs have been classified as carcinogenic (Figure 1) (Gabrieli et al. 2010).

Indeed, the earliest examples of occupational cancer were among chimney sweeps, iron foundry

workers and workers exposed to coal-tar products during the industrial revolution. Since then

these cancers are agreed to be the result of exposure to polycyclic aromatic hydrocarbons

(Gabrieli et al. 2010). As described by Phillips, PAHs are formed by the incomplete combustion

of carbon including burning of fossil fuels, smoking of tobacco and grilling or smoking of food

(Gabrieli et al. 2010). For non-smokers over 96% of PAH exposure is through the diet (Phillips 1999)
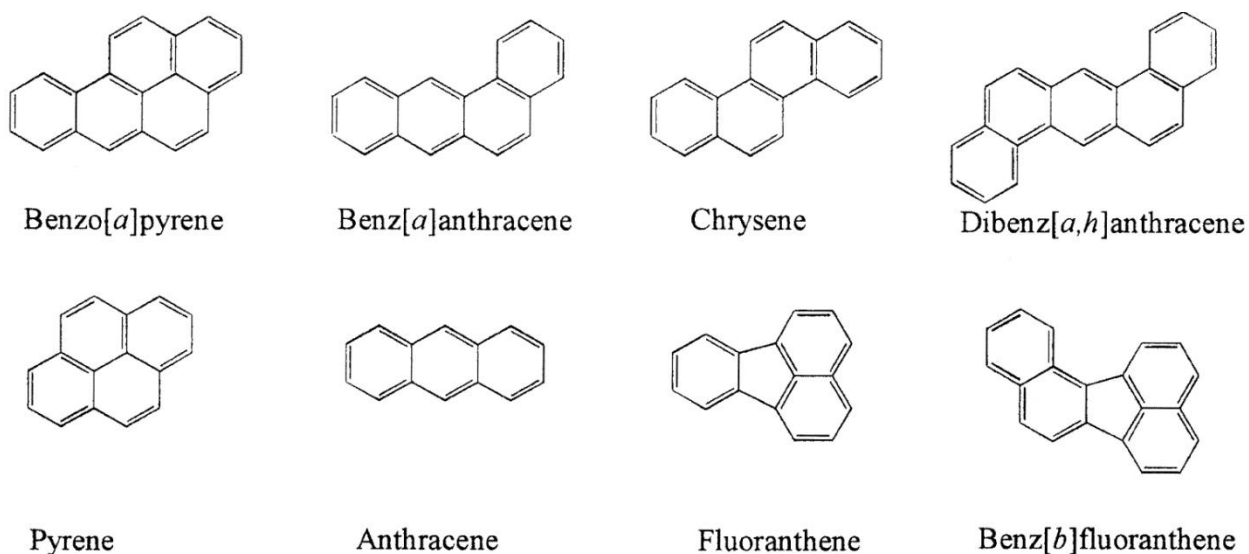
Fig. 1: Structures of some polycyclic aromatic hydrocarbons present in the environment and detected in food. (Figure from Phillips, 1999)

Smoking of food, a prime example of incomplete combustion, forms PAHs. Cooking food over an open flame, such as barbequing, also forms PAHs. Pyrolysis of fats from dripping onto an open flame generate PAHs which are deposited back onto the meat. Smoked meat can contain 2.6-29.8 parts per billion (ppb) total PAH, with smoked fish ranging from 9.3-86.6 ppb (Phillips 1999).

Quantification of PAHs levels in an unindustrialized area of Japan established a baseline for fish at no detectable levels of PAHs and up to 3 ppb for shellfish. Molluscs harvested from polluted waters can reach levels well into the parts per million (ppm) range (Phillips 1999).

PAHs are also detected in a wide variety of plants. Leafy vegetables such as lettuce can contribute a significant amount of PAHs to the diet with some reported levels higher than that of cooked meat. Processed vegetable products, such as cereal, vegetable oil and margarine can contain even higher PAH levels. The main source of contamination in plants occurs from the deposition of small airborne particles containing PAH compounds. Contamination can also occur to a lesser extent through uptake from soil and endogenous biosynthesis.   PAH levels in plants are governed by growth location, with those grown near industrialized areas resulting in significantly increased PAH contamination (Phillips 1999).

PAHs occur in complex environmental mixtures and present a challenge for both measurement and determining the effects on the human body. As reviewed in Phillips, there are two main approaches for measuring PAHs in the environment and in complex matrices such as food. One approach involves the determination of 15-20 commonly detectable PAHs including carcinogenic and noncarcinogenic compounds. The other approach uses benzo[a]pyrene (B[a]P) measurements as a marker and surrogate for all PAHs. The first approach presents a detailed view of the overall relative amounts of PAHs. Phillips states that since more than half of the total PAHs constitutes noncarcinogenic or weakly carcinogenic PAHS, the measurement of benzo[a]pyrene, the most commonly found carcinogenic PAH, potentially gives a more biologically significant measure of PAH contamination (Phillips 1999).

Many PAHs are complete carcinogens as well as initiators, meaning in addition to their genotoxic mechanism of inducing mutations, they also have the ability to act as tumor promoters. Initiation is the transformation of a normal cell to a dormant cancer cell while promotion is the

expansion of that initiator cell into a group of tumor cells. PAHs have been shown to be complete carcinogens due to their ability to induce skin tumors in mice after repeated prolonged exposure (Baird, Hooven, and Mahadevan 2005). Animal studies have suggested that dietary intake of benzo(a)pyrene causes increased levels of tumors at several sites, particularly in the gastrointestinal tract (Sinha 2005).

After ingestion, inert lipophylic PAHs are converted to reactive electrophiles by CYP1A1 (cytochrome P450, family 1, subfamily A, polypeptide 1) and CYP1B1 (cytochrome P450, family 1, subfamily B, polypeptide 1) mono-oxygenases for conjugation and excretion from the cell (Baird, Hooven, and Mahadevan 2005). Other enzymes such as glutathione transferase (GST), uridine diphosphate (UDP), glucuronosyl transferase, epoxide hydrolase and methyl transferase also contribute to the detoxification of PAHs (Shimada 2006). However, this metabolism of PAHs can also create PAH diol epoxides capable of binding DNA and other macromolecules in the cell (Figure 2). The ability of PAH adducts to persist in genomic DNA to form mutations depends on the conformation of the adduct within the DNA sequence and the ability of DNA repair mechanisms, to identify and remove the lesions (Baird, Hooven, and Mahadevan 2005). Preliminary data from the Buermeyer lab also suggests the DNA mismatch repair pathway can modulate the mutagenicity of PAHs (A. Buermeyer and C. Kernan, unpublished).
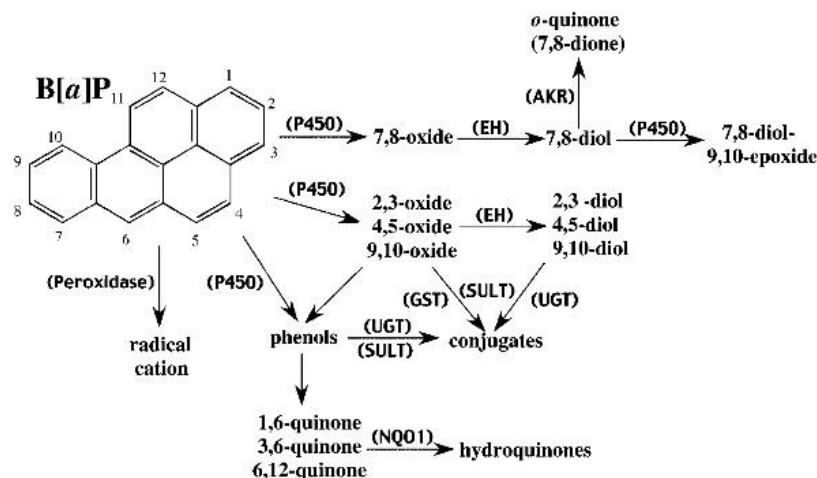
B[a]P

o-quinone
(7,8-dione)

(AKR)

(P450) → 7,8-oxide (EH) → 7,8-diol (P450) → 7,8-diol-9,10-epoxide

(P450) → 2,3-oxide / 4,5-oxide / 9,10-oxide (EH) → 2,3-diol / 4,5-diol / 9,10-diol

(Peroxidase) (P450)

radical cation

phenols (UGT)/(SULT) → conjugates

(GST) (SULT) (UGT)

1,6-quinone / 3,6-quinone / 6,12-quinone (NQO1) → hydroquinones

Metabolism of B[a]P by P450s and other xenobiotic-metabolizing enzymes. (P450, cytochrome P450; EH, epoxide hydrolase; GST, glutathione transferase; UGT, UDP-glucuronosyltransferase; SULT, sulfotransferase; NQO1, NAD(P)H-quinone oxidoreductase 1; and AKR, aldo-keto reductase).

Figure 2: Metabolism of B[a]P by P450s and other xenobiotic-metabolising enzymes. (Figure from Shimada, 2006)

DNA Mismatch Repair

DNA Mismatch repair (MMR) operates during DNA replication to prevent the development of mutations by degrading error-containing sections of a newly synthesized DNA strand, and thereby allowing DNA polymerases another opportunity to generate an error-free copy of the template sequence. To function properly MMR complexes must be able to efficiently recognize base-base mismatches and insertion/deletion loops (IDLs) and must direct the repair machinery to the newly synthesized DNA strand that includes the faulty genetic information (Jiricny 2006) (Table 1). In the absence of MMR activity, DNA polymerase errors generated during DNA replication are allowed to persist in DNA, leading to the generation of mutations. An accumulation of mutations in cells lacking MMR promotes the transformation of individual cells leading to the development of cancer (Jiricny 2006). The extent to which environmental factors also contribute to, or enhance, cancer risk in MMR-deficient individuals is not known.

Distribution of MMR proteins.

Molecular function	Thermus thermophilus	Escherichia coli	Saccharomyces cerevisiae	Homo sapiens
Mismatch recognition	MutS	MutS	MutSα (MSH2/MSH6) MutSβ (MSH2/MSH3)	MutSα (MSH2/MSH6) MutSβ (MSH2/MSH3)
Strand incision	β-clamp[*1] clamp-loader[*1] MutL	—	PCNA RFC MutLα (MLH1/PMS1) MutLγ[*2] (MLH1/MLH3)	PCNA RFC MutLα (MLH1/PMS2) MutLγ[*2] (MLH1/MLH3)
Strand incision	—	MutH	—	—
Match making	MutL	MutL	MutLα (MLH1/PMS1) MutLβ (MLH1/MLH2) MutLγ (MLH1/MLH3)	MutLα (MLH1/PMS2) MutLβ (MLH1/PMS1) MutLγ (MLH1/MLH3)
Strand excision (single-stranded DNA-binding)	SSB	SSB	RPA	RPA
Strand excision (exonuclease)	RecJ ExoI	RecJ ExoI ExoVII ExoX	EXO1[*3]	EXO1[*3]
Strand excision (helicase)	UvrD	UvrD	—	—
Repair synthesis	DNA polymerase III	DNA polymerase III	DNA polymerase δ	DNA polymerase δ

[*1]The involvement of bacterial clamp and clamp-loader in the strand incision reaction has not yet been confirmed. [*2]It is demonstrated that the endonuclease motif in MLH3 is responsible for *in vivo* MMR [83]; however, the endonuclease activity of MutLγ has not yet been confirmed biochemically. [*3]In yeast and human, EXO1 has the 5′-flap endonuclease activity in addition to 5′–3′ exonuclease activity.

Table 1: Distribution of MMR proteins. (Table from Jiriciny, 2006)

The MMR pathway can be divided into three principle steps: recognition of mispaired bases, excision where the error-containing strand is degraded resulting in a gap, and repair synthesis where the gap is filled by the DNA polymerase (Mathews, Cabarcas, and Hurt 2012) (Figure 3). MMR activity begins with mismatch recognition by the MutSα or by MutSβ protein complexes. MutSα and MutSβ are heterodimers, complexes comprised of two different, but related, proteins. MSH2 and MSH6 proteins comprise MutSα while the MSH2 and MSH3 proteins comprise MutSβ (Hernandez-Pigeon et al. 2004). MutSα initiates the repair of base-base mismatches and small IDLs while MutSβ initiates repairs of larger IDLs. Since both complexes contain MSH2, mammalian cells lacking MSH2 lack all mismatch recognition functions and are completely MMR-deficient (Jiricny 2006).

As reviewed by Mathews et al, formation of the MutS-DNA complex is followed by ATP-dependent recruitment of MutL homolog complexes. MutL complexes couple the recognition of mispaired bases by the MutS complexes to downstream MMR events, which lead to the removal of the strand containing the error. Three MutL activities have been identified. MutLα, a heterodimer of MLH1 and PMS2, is responsible for approximately 90% of MutL activity in humans and supports the repair initiated by both MutS complexes. Two additional MutL heterodimers, MutLβ and MutLγ, comprising MLH1/PMS2 and MLH1/MLH3 respectively, may play minor roles in mismatch repair (Mathews, Cabarcas, and Hurt 2012).

Assembly of the MutS-MutL-DNA heteroduplex ternary complex is required for activation of exonuclease mediated degradation of the error-containing strand. Exonuclease 1 (EXO1) degrades the error containing strand through a 5' to 3' exonucleolytic activity (Mathews, Cabarcas, and Hurt 2012). The gap left by EXO1 is resynthesized by DNA polymerase δ, which is accompanied by a proliferating cell nuclear antigen (PCNA) and replication protein A (RPA). MMR is completed by DNA ligase I sealing the remaining nick (Mathews, Cabarcas, and Hurt 2012).
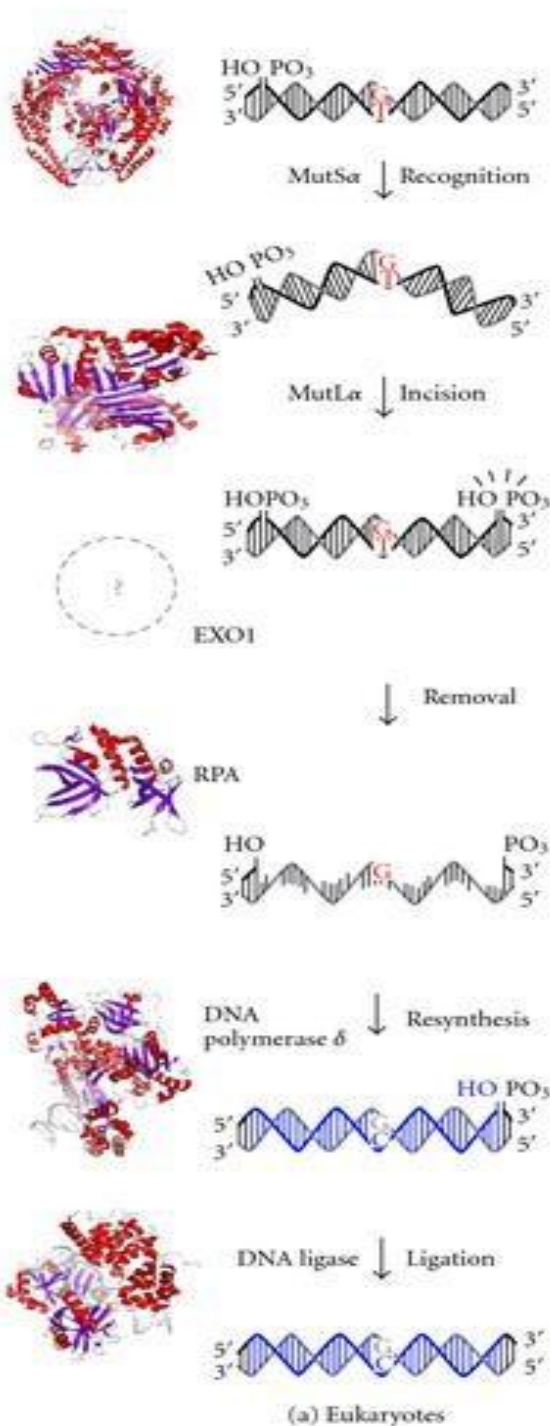
Figure 3: A schematic representation of MMR pathway models. Eukaryotic MMR. A DNA mismatch is generated by the misincorporation of a base during DNA replication. Mu t S α recognizes base-base mismatches and M u t L α nicks the 3' or 5' side of the mismatched base on the discontinuous strand. The resulting DNA segment is excised by the EXO1 exonuclease, in cooperation with the single-stranded DNA-binding protein RPA. The DNA strand is resynthesized by DNA polymerase δ and DNA ligase 1. (Figure from Fukui, 2010)

Genetic Factors in CRC

Since colorectal cancer occurs mainly in older individuals, the theory is that a cell must accumulate several different mutations leading to the activation of oncogenes, genes with the potential to cause cancer, and the inactivation of tumor-suppressor genes, in order to undergo malignant transformation (Midgley and Kerr 1999). If one or more defects are present at birth as inherited genetic abnormalities then fewer mutations are required for disease onset.

Approximately 15% of colorectal cancers occur in the context of an inherited cancer predisposition syndrome (Kinzler and Vogelstein 1996), whereas approximately 30% of CRC cases involve patients with a family history of CRC (Siegel and Jemal 2014). According to Kinzler and Vogelstein, 1996, two main inherited syndromes are associated with colorectal cancer: familial adenomatous polyposis (FAP) and Lynch Syndrome or hereditary non-polyposis colorectal cancer (HNPCC). FAP is identified by a mutation in the adenomatous polyposis coli (ACP) gene on chromosome 5q21. The specific mutation and resulting tumor locations vary from patient to patient. Truncating mutations between codons 463 and 1387 are associated with retinal lesions while truncating mutations between codons 1403 and 1578 are associated with desmoid tumors and mandibular lesions. Though not all patients show the same symptoms, they typically develop hundreds to thousands of colorectal adenomas during their 20s and 30s (Kinzler and Vogelstein 1996).

Lynch Syndrome

As reviewed by Midgley and Kerr, mutations in the MutS homolog, MSH2, involved in the mismatch repair pathway, were demonstrated to cause to Lynch Syndrome. In subsequent research, mutations in the *MSH2* gene have been shown to account for approximately 60% of

Lynch Syndrome cases. In addition, mutations affecting *MLH1*, *PMS1*, and *PMS2* have been

identified as accounting for 30%, 5% and 5% of Lynch Syndrome cases, respectively. Deficient

mismatch repair produces an identifiable genetic marker in the associated cancers, namely

microsatellite instability. With dysfunctional MMR, mismatched loops caused by replication

errors are undetected and uncorrected, resulting in mutations that can affect gene function. For

example, evidence suggests these loops can cause mutations in the tumor growth factor β

receptor (RII) which acts as a tumor-suppressor gene in colon cells. With mutations that

inactivate RII, cells are allowed to grow unchecked. More than 90% of patients with

microsatellite instabilities exhibit inactivating mutations in RII (Midgley and Kerr 1999).

Sporadic CRC

Colorectal cancer does not solely come from inherited genetic diseases. In fact, most

colorectal cancers arise sporadically, meaning there is no obvious pattern of inheritance that

could be attributed to an inherited genetic disease that caused the cancer (Jasperson et al. 2010).

Some sporadic CRCs are the result of somatic hypermethylation of the *MLH1* promoter region.

However, as mentioned above, sporadic CRC risk does increase in individuals with a family

history of cancer, suggesting that unknown genetic factors, potentially polymorphic variants

affecting multiple genes, do contribute to cancer risk. The extent to which, and the identity of,

polymorphic variations in the genome of different individuals contribute to the development of

cancer in different individuals is unknown. Furthermore, it is likely that specific combinations of

environmental exposure and genetic deficiencies will interact to increase cancer risk (Jasperson

et al. 2010).

Experimental Objectives and Rationale

Cancer results from a combination of environmental and individual genetic risk factors (Jasperson et al. 2010). To identify an individual person's risk of developing cancer we must understand the biological pathways that influence how the body responds to environmental exposures that affect cancer risk. Importantly, we must also understand how variation in the inherent capacity of different cellular pathways affects risk from different environmental exposures. The Buermeyer laboratory is interested in indentifying environmental agents, exposures and lifestyle choices that might specifically increase cancer risk in individuals with inherited or genetic MMR deficiencies. Of particular interest are PAHs.

To indentify exogenous factors that might interact with MMR deficiencies, past studies have taken several different types of approaches to measure the impact of specific genetic deficiencies in MMR, and the effect of different exposures on the phenotype of cells with MMR deficiencies. Examples of past methods, outlined in Rasmussen et. al, include measuring cellular response to methylating and other DNA damaging agents, measuring the spontaneous mutation rate at the endogenous *HPRT* gene, and measuring microsatellite instability. A limitation with all of these methods is the choice of cells studied. Most cell-based studies use a human cancer cell line that has lost expression of the endogenous MMR protein. These MMR-deficient cells provide a model for testing the ability of a MMR gene to restore repair function compared to a normal, healthy wild-type cell. However, due to the loss of MMR function, these cell lines have undergone multiple replication cycles of mutation and selection, creating a variable and uncertain genetic background that may affect the outcome of experimental procedures (Rasmussen et al. 2012).

Considering this, the objective of this research was to create an improved model system with which to perform functional assays for MMR capacity. I theorized that by starting with MMR-proficient cells and transfecting the cells with short-interfering RNA (siRNA) specific for MMR genes, I could limit the expression of specific MMR proteins resulting in a disruption of MMR activity. I chose siRNA due to its selective inhibition of target protein expression (Schütze 2004). Ideally, this approach would create isogenic cell cultures deficient in different specific mismatch repair proteins. Such cultures would not have experienced multiple replication cycles with an inherently and significantly elevated spontaneous mutation rate, thus avoiding the accumulation of multiple mutations as seen with MMR-deficient cancerous cell lines. The HeLa cell line was chosen for its short replication period.

MMR primarily depends on the activities of two critical protein heterodimers, MutSα, comprised of MSH2 and MSH6, and MutLα, comprised of MLH1 and PMS2, with some backup activity provided by MutSβ, comprised of MSH2 and MSH3, and MutLβ, comprised of MLH1 and MSH3. As MSH2 and MLH1 are obligate components of the MutS and MutL complexes, respectively, deficiency in either protein can result in a complete inactivation of MMR. I therefore chose to compare targeting either MSH2 or MLH1 for knockdown by transfection with siRNA, using commercially available siRNA specific for either gene.

To measure the effect of siRNA-mediated inhibition of MMR gene expression, I chose a functional assay for MMR activity that involved 6-Thioguanine cytotoxicity. Cytotoxicity of 6-TG at relatively low doses requires functional MMR, including MLH1 and MSH2 protein activities. The mechanism of MMR-dependent cytotoxicity following 6-TG exposure involves the recognition of methylated thioguanine bases incorporated into DNA and subsequently mispaired with thymine during DNA replication. Recognition and binding of such mispaired

thioguanine lesions during replication triggers a MMR-dependent DNA damage response that can lead to activation of cell death pathways, including apoptosis. The DNA damage response requires both MutSα and MutLα, and can be used as a measure of the cell's capacity for MMR. Cells lacking MMR avoid triggering the cytotoxic response and are significantly resistant to cell killing induced by 6-TG.

siRNA

SiRNAs are approximately 21-23 nucleotides long, often with symmetric 3' and 5' ends, that can be produced by cutting long double-stranded RNAs (dsRNAs) with RNase III family enzymes, or Dicer. When transfected into mammalian cells via a lipid-based transfection system, siRNAs are able to effectively silence endogenous genes (Schütze 2004). Once present in the cytoplasm, the siRNA is incorporated into a protein complex called the RNA-induced silencing complex (RISC) which seeks out and degrades messenger RNA (mRNA) complementary to the antisense siRNA strand, propogating silencing of the specific gene (Whitehead, Langer, and Anderson 2009).

Transfection of mammalian cells with siRNA using lipid-based transfection reagents to reduce expression of specific target genes is critically dependent upon cell density and the growth rate and overall health of the cell culture. Optimal cell density for transfection can be cell line dependent, but generally is approximately 50 to 75% confluency. If the cell density at the time of transfection is too low, approximately 30 to 40% confluency, toxicity caused by the transfection reagent can limit the growth and survival of the cell culture and thus interfere with any subsequent functional analysis of cell phenotype. Cultures that are too confluent can lead to reduced measured transfection efficiency and therefore a reduced inhibition of gene expression.

In addition, too dense a culture at the time of transfection can limit the time available for functional assays that require multiple days of cell growth, as the transfected cultures become confluent with an associated reduction in the health of the cells. The initial experiments, described below in the Results and Discussion, were designed to identify optimal plating conditions for successful transfection.

Experimental Approach

The ultimate goal with my approach is to use the isogenic cell cultures created by using siRNA transfection to address the extent to which environmental carcinogens, such as PAHs, interact with specific MMR deficiencies to increase the accumulation of mutations, and therefore the risk of cancer. This thesis reports the results of experiments testing the hypothesis that siRNA transfection is a useful approach for establishing isogenic cell cultures with MMR deficiencies. MMR status following transfection with siRNA targeting either MSH2 or MLH1 was assessed by measuring MLH1, MSH2 and MSH6 protein accumulation and the MMR-dependent cytotoxic response to 6-Thioguanine (6-TG) in the MMR-proficient HeLa cell line. Surprisingly, I detected a differential effect on MMR protein accumulation versus apparent MMR activity. Although significant reductions in MLH1, MSH2 and MSH6 were detected, I measured no altered capacity for triggering the MMR-dependent cytotoxic response to 6-TG in siRNA-transfected HeLa cultures. As discussed below, issues associated with the experimental design of the cytotoxicity assay may have interfered with detection of any reduction in MMR activity. Additional work is needed to determine whether siRNA-mediated inhibition of MMR gene expression is a viable basis for an assay that measures MMR capacity.

Materials and Methods

Cell Culture

HeLa cells, purchased from American Type Culture Collection (ATCC) (Manassas, VA), were routinely maintained as sub-confluent cultures under sterile conditions in 37° C humidified incubators with 5% atmospheric CO_2. New cultures, following the initial thaw of frozen stocks, underwent a minimum of one week's maintenance prior to use in experiments. Dulbecco's Modified Eagle's Medium (DMEM) (Cellgro, Manassas, Virginia) supplemented with 10% heat-inactivated fetal bovine serum (FBS) (Tissue Culture Biologicals, Long Beach, California) was used for maintenance. Trypsin (Gibco, Carlsbad, California) was used to remove cells from plates during subculture. Cell counts using a hemocytometer and trypan blue stain distinguished viable from nonviable cells.

siRNA Transfection

Cells were plated at a density of 1.5×10^5 cells per well into 6-well tissue culture plates along with 3 mL of DMEM complete medium. After a 24 hour recovery period the complete medium was aspirated and the wells rinsed with isotonic phosphate buffered saline (PBS) (Hyclone, Logan, Utah). Cells then underwent transfection with 20 nmol diluted siRNA (Qiagen, Valencia, California) (Anti-MSH2 siRNA, Cat# Si02663563) (Anti-MLH1 siRNA, Cat# SI02662072) (Allstars Negative Control siRNA +AF488, Cat# 1027292) as per manufacturer's instructions using the "Fast-Forward" protocol. Allstars negative siRNA is tagged with a fluorescent light emitting molecule that can be detected with the proper wavelength of light. 4 µl siRNA was diluted into 36 µl of RNAse free water. 36 µl of the diluted siRNA solution was removed and mixed with 564 µl of serum-free DMEM medium and 72 µl Hiperfect transfection reagent (Cat # 301705, Qiagen, Valencia, California). The solution was incubated for 10 minutes at room temperature to allow the transfection complexes to form.

112 μl of the solution was subsequently added dropwise into each well of the 6-well plate. Cell cultures were returned to humidified incubators and incubated for 24 hours before the transfection medium was replaced with DMEM complete medium. Cells were subcultured at 48 hours post-transfection to maintain optimal confluency.

Flow Cytometry

Cell cultures transfected with Allstars Negative control siRNA were harvested, at 24 hours post-transfection with trypsin, collected by low speed centrifugation and resuspended in PBS. To fix cells, 100% ethanol was added dropwise to a final concentration of 70% ethanol (v/v). Fixed cells, stored at -20° for a minimum of 12 hours, were stained with propidium iodide for analysis of siRNA content. To increase membrane permeability, fixed cells were washed twice and suspended in a PBS solution of 0.1% Triton (Dow Chemical, Midland, Michigan). A solution of 200 pg/mL RNAse and 20 ng/mL propidium iodide was added to treat the cells followed by a 30 minute incubation at 37° C. The cellular suspension was then filtered through a 37-micron mesh cloth, removing large aggregations of cells, and stored in a titer tube for cell-cycle analysis by the Cytomics FC 500 machine (Beckman Coulter, Brea, California). Allstars Negative siRNA content analysis was accomplished with the help of the EHSC core facility and Sam Bradford at Oregon State University via the flow cytometry analysis software programs MultiCycle and FlowJo VS 10.0.2 (Tree Star, Ashland, Oregon).

Whole Cell Lysates

Harvesting of cells for preparation of whole cell protein lysates occurred at 24, 48, 72 and 96 hours post-transfection as specified. Cells were harvested into 15 mL conical tubes and pelleted by centrifugation. Resuspension with 5 mL cold 1x PBS and a second subsequent pelleting by centrifugation ensured that the DMEM media was completely removed from the cell suspension. Following the second centrifugation 5 "pellet volumes" (i.e, five times the pellet's

volume estimated by visual comparison against known volumes of water in the same tube type)

of PBS were used to re-suspend the pellet. Cells were lysed using 5 "pellet volumes" of a 2x

lysis buffer containing 100 mM Tris-HCL, 4% sodium dodecyl sulfate (SDS) and 20% glycerol

to which a protease inhibitor cocktail tablet (Complete Mini EDTA-Free, Roche Diagnostics,

Indianapolis, Indiana) had been added. Lysed cells were heated to approximately 95° C followed

by snap-freezing in liquid nitrogen, and stored at -80° until use.

BCA Assay

A colorometric Bicinchoninic Acid (BCA) Assay (Thermo Fisher Scientific, Rockford,

Illinois), administered according to manufacturer's instructions, was used to determine the

protein concentration of the whole cell protein lysates. Bovine serum albumen (0 µg/mL) was

used to generate a standard curve. A SpectraMax 250 (Molecular Devices, Sunnyvale,

California) along with the SoftMax Pro 3.1.1 program (Molecular Devices, Sunnyvale

California) measured protein absorbance at 538 nm. Interpolation based on linear regression of

absorbance values for the standard curve determined the protein concentrations of the lysates

which were plotted using Prism 5.0d (Graph Pad Software, La Jolla, California).

Immunoblotting after SDS-Polyacrylamide Gel Electrophoresis

Separation of proteins was accomplished via denaturing gel electrophoresis. Tris-HCL

gels (7.5%, Bio-Rad, Hercules, California) along with the running buffers 1x XT MOPS (n-

morpholino-propane-sulfonic acid) (Bio-Rad) and 19.2 mM glycine and 2.5 mM Tris base (with

0.1% SDS per manufacturer's instructions) were used for electrophoresis. 50 µg of protein was

loaded into each lane and electrophoresed with 200 volts (constant voltage) for 50-55 minutes.

Proteins were then transferred to a polyvinylidene fluoride (PVDF) membrane (EMD Millipore,

Billerica, Massachusetts) using the submerged transfer protocol (as per manufacturer's instructions) at a constant voltage of 100 V for 55 minutes in a Criterion Blotter (Bio-Rad). A transfer buffer of 10% v/v methanol, 19.2 mM glycine and 2.5 mM Tris base in nanopure water was used to facilitate transfer. Membranes were left to soak overnight at 4^0C in a blocking solution of 25 mM Tris, 137 mM NaCl (sodium chloride), 27 mM KCL (potassium chloride), and 0.1% Tween 20 (TBST) with 5% w/v of dry powdered milk post-transfer to suppress nonspecific antibody binding. Membranes were then probed sequentially with the commercially available mouse monoclonal primary antibodies: anti-MSH6 used at a concentration of 2.0 µg/mL (Cat#: 610918, BD Biosciences, San Jose, California), anti-MLH1 at a concentration of 1 µg/mL (Cat#: 51-1327GR, BD Biosciences), and anti-MSH2 at 0.2 micrograms/mL (Cat#: NA27, Calbiochem, San Diego, California). Following incubation, excess primary antibody was removed by washing the membranes in TBST four times for fifteen minutes each for a total time of one hour. Membranes were then incubated at room temperature for one hour with horseradish-peroxidase-conjugated (HRP) goat-anti-mouse secondary antibody (Cat#: 31430, Thermo Fisher Scientific) at a concentration of 10 µg/mL and HRP modified streptavidin (5000x StrepTactin, Bio-Rad) at a concentration of 0.2 µL/mL.   Membranes were then washed twice with TBST and twice with TBS for fifteen minutes each for a total of 1 hour.

Imaging/Analysis

Indirect visualization of primary antibodies was accomplished using Supersignal West Pico Chemiluminescent Substrate Kit (Thermo Fisher Scientific) as per manufacturer's instructions. A ChemiGenius Imager (Syngene, Frederick, Maryland) with the software program GeneSnap (Syngene) was used to capture images. Images were analyzed using the program GeneTools (Syngene).

Cytotoxicity with HPRT and 6-TG

MMR function post-transfection was analyzed using clonogenic survival following exposure to the cytotoxic purine analog, 6-thioguanine (6-TG). 500 cells were plated into 100 mm dishes and allowed to recover overnight before exposure to 6-TG at concentrations of either 0, 0.1, 0.3, 1.0, or 3.0 µM. Two replicates were plated for each dose and harvesting time (see figure legends). Colonies were allowed to form for 12 to 14 days before plates were fixed and stained using methylene blue dye (Sigma, St. Louis, Missouri) in 2% ethanol, and subsequently counted by visual inspection. The two replicate plates for each dose and harvesting time were averaged and normalized to the counts from the 0 dose plates, and expressed as a percentage.

Results and Discussion

To create an improved model system with which to perform functional assays for MMR I transfected cultures of a MMR-proficient cell line, HeLa, with short-interfering RNA (siRNA) specific for two different, essential MMR genes, MSH2 and MLH1. To identify the optimal conditions for successful "knockdown", or inhibition, of MSH2 and MLH1 with siRNA, I first performed several experiments varying the initial cell plating density.

HeLa cells from an exponentially growing stock culture were plated at various densities in standard 6-well culture dishes and monitored daily for up to one week after plating. Examination of cell survival and growth by phase-contrast microscopy (data not shown) demonstrated that wells plated with $2.0*10^5$ and $2.5*10^5$ cells yielded cultures that became over-confluent after one day of growth post plating whereas plating $1.0*10^5$ cells per well led to cultures with too low a cell density, approximately 20% confluency. The wells plated with $1.5*10^5$ cells reached confluency at approximately two days, which should allow sufficient time for the siRNA transfection while also providing a sufficient density of cells for successful transfection. Similar results were seen in a repeat of the experiment (data not shown). I concluded that plating $1.5*10^5$ cells per well yielded the optimal cell density for subsequent siRNA transfection.

To measure the percentage of cells in the transfected cultures that successfully took up the siRNA I transfected HeLa cells, plated as described above, with a siRNA tagged with a fluorescent light emitting molecule. Analysis of transfected cells by flow cytometry revealed an

uptake percentage of approximately 37% of the cells in the culture. I suspect the percentage of cells successfully transfected in this experiment may appear artificially low due to the improper storage of the siRNA, which would decrease the light-emitting capacity of the fluorescent molecule. I was unable to repeat this experiment due to the inactivation of the siRNA.

Cells were harvested at various times after transfection for preparation of cell-free protein extracts and subsequent analysis by immunoblotting. To determine the effectiveness of siRNA transfection for limiting MLH1 or MSH2 protein accumulation in HeLa cells I transfected cell cultures, plated as described above, with anti-MLH1 siRNA or anti-MSH2 siRNA. Negative controls were parallel cultures transfected with a negative control siRNA or remained untransfected. The cellular abundance of MLH1, MSH2 and MSH6 was analyzed by protein immunoblotting using whole cell lysates of the transfected cells harvested at 24 hours or 48 hours after transfection (Figures 4a-d). Semiquantitative analysis of the resulting digital image demonstrated a reduction in protein accumulation of MLH1, MSH2 and MSH6 relative to untransfected and negative control-transfected cells. Cells transfected with siRNA targeting MLH1 demonstrated a reduction in MLH1 protein accumulation of approximately 30% at 24 hours post transfection and approximately 70% at 48 hours post transfection. Cells transfected with anti-MSH2 siRNA demonstrated approximately 20% reduction in protein accumulation of MSH2 at 24 hours post transfection and 70% reduction in protein accumulation of MSH2 at 48 hours post transfection. In cells transfected with anti-MSH2, MSH6 protein levels also were reduced as expected due to MSH2's role in stabilizing MSH6 during formation of the MutSα heterodimer. Importantly, there was no consistent reduction of MLH1 protein in anti-MSH2 transfected cells; similarly MSH2 and MSH6 were not reduced in anti-MLH1 transfected cells.

Together the results indicate that each specific siRNA is able to inhibit the production of its specific target protein in HeLa cells. The results also indicate that I have established the necessary cell culture conditions for successful transfection with the siRNAs of interest.

To determine the time course for inhibition of MSH2 protein, I transfected HeLa cell cultures with anti-MSH2 siRNA as before and harvested cells at various times post-transfection. Negative controls for the transfection were as described above. The cellular abundance of MSH2 and MSH6 protein was analyzed by protein immunoblotting using whole cell lysates of the transfected and control cells as above (Figures 5a-d). Analysis of the resulting immunoblot revealed reduced protein accumulation of MSH2 relative to untransfected and negative control-transfected cells in both the 48 and 72 hour post-transfection samples. As found in initial transfection (Figure 4), MSH6 protein levels also were reduced in the same samples. MSH2 protein levels appeared to be somewhat higher in the sample harvested 96 hours post-transfection, suggesting the time period in which the siRNA is most successful in limiting production of MSH2 is approximately 48 to 72 hours post-transfection.   Based on these initial transfections, I concluded that the anti-MSH2 siRNA is effective in HeLa cells at significantly limiting the cellular accumulation of MSH2 and MSH6 and therefore the MutSα heterodimer complex, for a period spanning approximately 48 to 72 hours post-transfection. As MutSα is the primary mismatch and DNA lesion recognition protein complex for MMR, the reduction in cellular abundance of MutSα is predicted to result in decreased MMR activity during the same time frame. Therefore, I next sought to determine the impact on MMR following transfection with anti-MSH2 siRNA in HeLa cells.

To determine the effect of reduced MSH2 protein accumulation on the MMR capacity of HeLa cells post-transfection, I measured the survival of cells after exposure to the purine analog 6-thioguanine (6-TG). I anticipated that cultures with reduced MSH2 protein accumulation would have significantly increased survival compared to the negative control and untransfected cultures when exposed to 6-TG (Figure 6A). HeLa cells transfected with anti-MSH2 siRNA were exposed at various times post-transfection to the indicated concentrations of 6-TG (see legend to Figure 6). I tested a range of 6-TG concentrations in order to identify any partial loss of cytotoxicity due to decreased MSH2 levels. Analysis of the resulting colony counts revealed that the untransfected cells and cells transfected with Allstars Negative control siRNA responded as expected to 6-TG exposure, demonstrating decreased cell survival as the 6-TG exposure dose increased (Figures 6a-e). Surprisingly, cells transfected with anti-MSH2 siRNA did not respond as expected and demonstrated no significant difference in survival between the anti-MSH2 transfected cultures and cultures transfected with Allstars Negative control siRNA or the untransfected cultures. I had expected that the anti-MSH2 siRNA transfected cultures would survive 6-TG exposure due to decreased MMR capacity associated with the decreased levels of MSH2 and MSH6 seen in immunoblotting of whole cell lysates (Figure 5). These results suggest that MMR was functional despite lower MutSα levels, at least as measured in this assay (Figure 5). There are at least two possible interpretations of these results. First, it is possible that the MMR pathway was not affected by the reduced levels of MSH2 and MSH6, which could suggest that MutSα protein complex is present in significant excess in cells. Alternatively, our results may show no effect on MMR activity due to limitations of the assay. In my experiment, 6-TG remained in the culture medium for the entire colony growth period, potentially a problem given the relative stability of 6-TG in aqueous medium, and the apparently transient reduction in

MutSα levels (Figure 5). It is possible that MMR activity was initially inhibited. However increased MSH2 protein accumulation by 96 hours, and beyond, might have led to restored MMR while significant concentrations of 6-TG remained, resulting in re-activation of the MMR-dependent cytotoxic response. If true, colony formation measured 14 days after exposure might not report the loss of a MMR-dependent cytotoxic response to 6-TG, as initially surviving cells might have subsequently died as MMR activity increased, preventing the formation of visible colonies. An alternate approach would be to use a pulse exposure to 6-TG and/or a shorter-lived cytotoxic agent such as the alkylating agent N-methyl-N'-nitro-N-nitrosoguanidine (MNNG). It also would be possible to measure cytotoxicity by using a different assay, one that doesn't require a 14 day growth period for the formation of visible colonies. For example, CellTox Green (Promega, Madison, Wisconsin) is an assay for cytotoxicity based on detection of released biomarkers into the media, that might be used to demonstrate a transient increase in survival shortly after treatment with 6-TG or MNNG. One final potential problem with the colony forming assay as a measure of cytotoxic response is that the assay is not a very precise measure of cellular response. As an indirect measure of activation of the DNA damage response signaling pathway, there can be significant variation in the quantitative response from assay to assay leading to relatively large error bars and an inability to detect quantitatively small changes in the survival of a given culture. Relative imprecision for measuring modest effects on survival is potentially exacerbated by the possibility that not all cells in culture are responding equally. With a transient transfection, the amount of siRNA each cell in the culture receives, and therefore the extent of inhibition of MMR protein accumulation likely varies. Protein immunoblotting using whole cell extracts of pooled cells from each culture measured an average percent inhibition of approximately 70%. This average response may include, at the extremes,

some cells that took up very little siRNA and therefore experienced little or no inhibition of MMR, and some cells that experienced complete inhibition of MMR due to a greater uptake of siRNA. Variability in percent inhibition of MMR among the cells in the 6-TG exposed cultures could increase the inherent variability in colony forming assays and further mask any modest effects on survival.

In summary, experiments presented in Figures 4-5 demonstrate a consistent reduction in MSH2 and MSH6 levels 48-72 hours following transfection without a corresponding decrease in apparent MMR activity. Based on the several different, potentially compounding, technical isues associated with the 6-TG cytotoxicity assay, I hypothesize that MMR activity likely is reduced in cells with significantly reduced MutSα levels. Given that siRNA inhibition of MSH2 accumulation was most effective between 48 and 72 hours post transfection and the ineffectiveness of the cytotoxicity experiment utilizing 6-TG to detect decreased MMR activity, the best course of action would be to continue with siRNA transfections but to limit the 6-TG to a pulse exposure. The untransfected and negative control siRNA-transfected cells exhibited the proper response when exposed to 6-TG, indicating that aspect of the assay is performing as expected. Re-activation of MMR activity, due to the siRNA's transient inhibition of target proteins, coupled with 6-TG remaining active in solution, is likely the cause of the unexpected cytotoxic response of cell cultures transfected with anti-MSH2 siRNA. My results showed the siRNA transfection was an effective method to reduce levels of target MMR proteins. Limiting exposure of transfected cells to 6-TG for the relatively short time of 24 hours would remove the threat of 6-TG remaining in solution after re-activation of MMR activity. With this approach, the transiently MMR-deficient cells (from transfection with anti-MSH2 siRNA), would be

expected to demonstrate increased survival relative to untransfected and negative control transfected cells following exposure to 6-TG. Such results would be consistent with my hypothesis that significantly reduced amounts of MSH2 protein inhibit MMR activity. Future plans are to optimize transfection to increase the degree of protein inhibition and to refine our functional assays to measure the effects of reduced expression on MMR activity in response to DNA damage.

My original hypothesis, that siRNA transfection can effectively silence specific MMR gene expression to create MMR deficiencies and disrupt MMR activity, was partially supported. Immunoblotting of protein lysates from cell cultures transfected with anti-MSH2 and anti-MLH1 siRNA showed a decrease in target protein of approximately 60 to 70% between 48 and 72 hours post-transfection. However these same cultures with reduced MSH2 protein levels did not respond as expected when exposed to 6-TG. The anti-MSH2 transfected cultures, with reduced amounts of a critical MMR protein complex, MutSα, demonstrated an apparently normal, MMR-dependent, cytotoxic response to 6-TG exposure. Despite this, siRNA transfection shows promise as a viable method for generating isogenic cell cultures with varying deficiencies in MMR in order to investigate how PAHs and other environmental mutagens might interact with MMR deficiencies to influence risk of mutation, and by extension, risk of cancer. More work is needed to determine the extent of MMR capacity with the reduced levels of critical MMR proteins demonstrated herein.
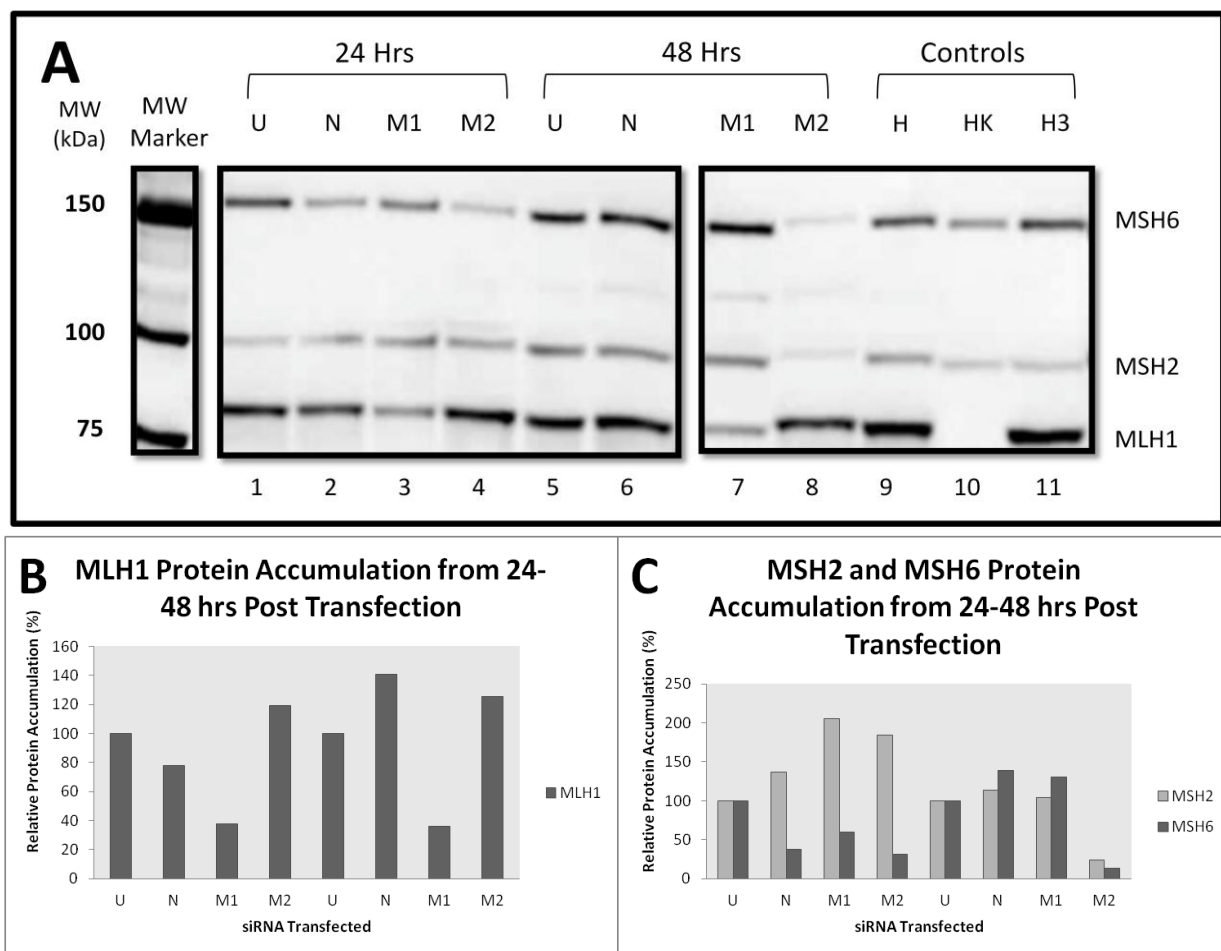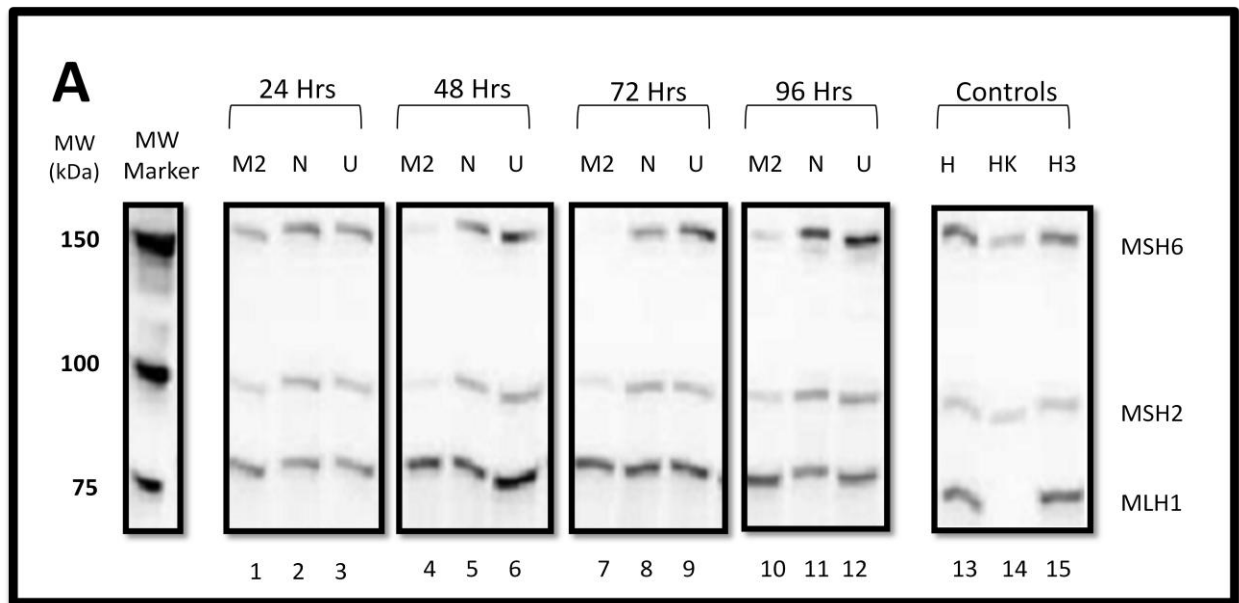
Figure 4: Accumulation of MLH1, MSH2 and MSH6 proteins in siRNA-transfected HeLa cultures. (A) The cellular abundance of MLH1, MSH2 and MSH6 proteins was determined by semi-quantitative protein immunoblotting of whole cell lysates prepared from HeLa cells transfected with anti-MLH1 siRNA (M1) or anti-MSH2 siRNA (M2). Negative controls were parallel cultures that remained untransfected (U) and parallel cultures transfected with Allstars Negative siRNA (N). Lysates of untransfected HeLa, HCT 116K, (a colon cancer cell line inherently deficient in *MLH1*) and HCT 116+hch3 (with restored MLH1) cell cultures served as loading controls, primarily to aid with identification of specific signals on the immunoblot. Plotted is the relative cellular abundance of (A) MLH1 or (B) MSH2 and MSH6 proteins as determined by semi-quantitative analysis of individual bands from the image in panel A. Band intensities were normalized to the signal from untransfected cultures harvested at the same time point. Labels are as described for Panel A. 100 percent in figures is the accumulation of specified protein in the untransfected sample at the specified time point.
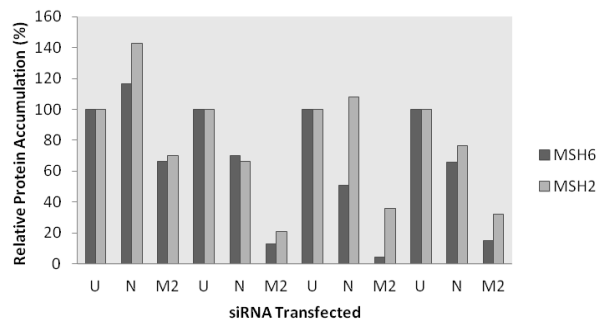
Figure 5: Accumulation of MLH1, MSH2 and MSH6 proteins in siRNA-transfected HeLa cultures. (A) The cellular abundance of MLH1, MSH2 and MSH6 proteins was determined by semi-quantitative protein immunoblotting of whole cell lysates prepared from HeLa cells transfected with anti-MSH2 siRNA (M2). Loading controls were the same as in Figure 4a. **(B)** and **(C)** are the same as in legend for Figure 4.
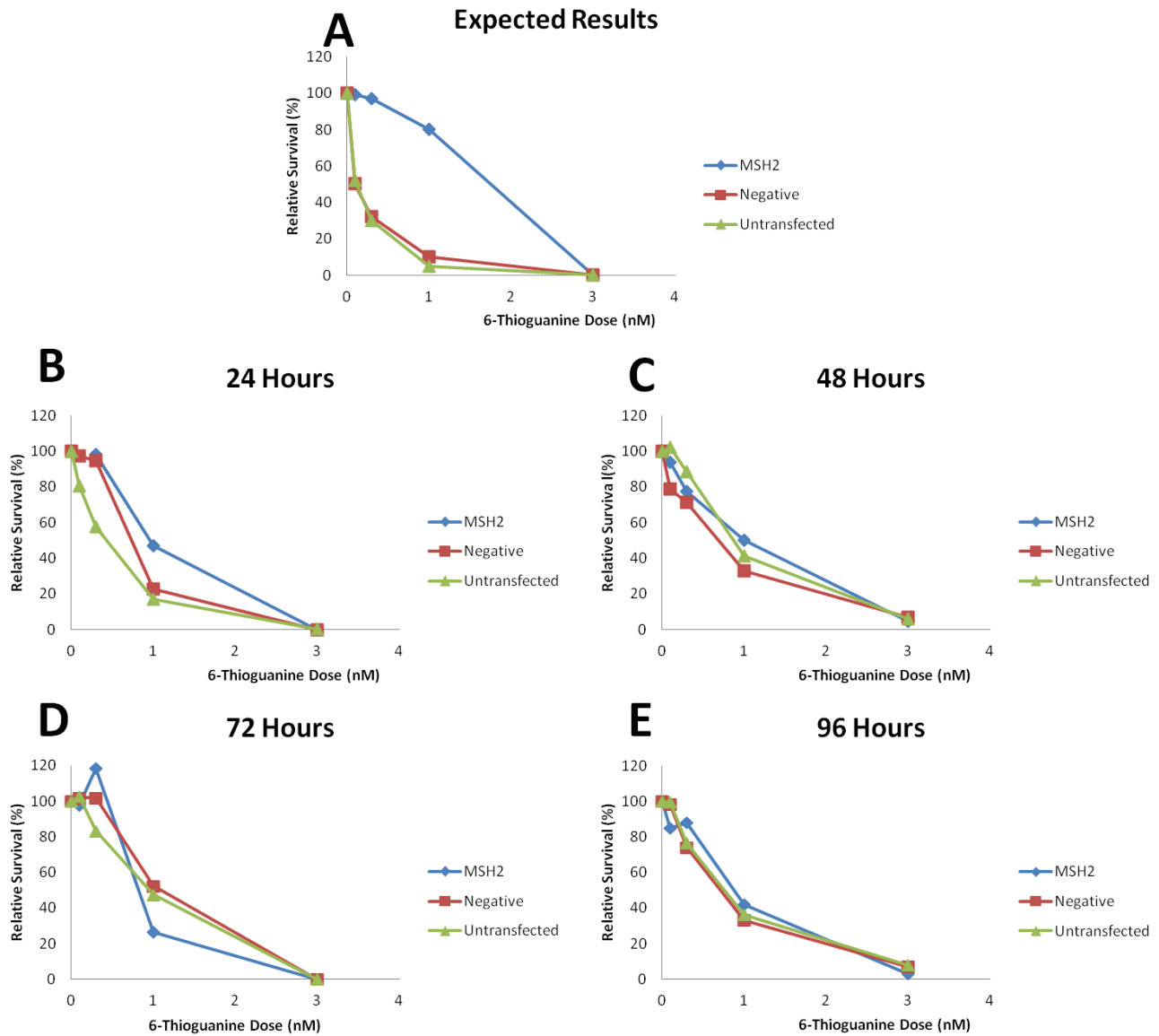
Figure 6: Mismatch Repair Dependent Cytotoxicity of 6-Thioguanine (6-TG) in HeLa Cultures Transfected with anti-MSH2 siRNA. To determine the effect of reduced MSH2 protein accumulation on the mismatch repair capacity of cells post-transfection, the survival of siRNA-transfected cell cultures was measured after exposure to 6-TG. Parallel cultures that remained untransfected and parallel cultures transfected with Allstars Negative siRNA served as controls. Cell cultures were exposed at the indicated times post-transfection to 0-3.0 nM 6-TG. **(A)** It was anticipated that cultures with reduced MSH2 protein accumulation would have significantly increased survival compared to the negative control and untransfected cultures when exposed to 6-TG. **(B-E)** Plotted is the relative survival of siRNA-transfected cultures exposed to the specified doses of 6-TG at the indicated times post-transfection. Relative survival, derived from counts of surviving colonies, was calculated as the surviving fraction normalized to the colony counts in unexposed cultures.

References

Baird, William M., Louisa A. Hooven, and Brinda Mahadevan. 2005. "Carcinogenic Polycyclic Aromatic Hydrocarbon-DNA Adducts and Mechanism of Action." *Environmental and Molecular Mutagenesis* 45 (2-3): 106–14. doi:10.1002/em.20095.

Bishehsari, Faraz. 2014. "Epidemiological Transition of Colorectal Cancer in Developing Countries: Environmental Factors, Molecular Pathways, and Opportunities for Prevention." *World Journal of Gastroenterology* 20 (20): 6055. doi:10.3748/wjg.v20.i20.6055.

Gabrieli, Jacopo, Paul Vallelonga, Giulio Cozzi, Paolo Gabrielli, Andrea Gambaro, Michael Sigl, Fabio Decet, et al. 2010. "Post 17th-Century Changes of European PAH Emissions Recorded in High-Altitude Alpine Snow and Ice." *Environmental Science & Technology* 44 (9): 3260–66.

Hernandez-Pigeon, Hélène, Guy Laurent, Odile Humbert, Bernard Salles, and Dominique Lautier. 2004. "Degadration of Mismatch Repair hMutSα Heterodimer by the Ubiquitin-Proteasome Pathway." *FEBS Letters* 562 (1-3): 40–44. doi:10.1016/S0014-5793(04)00181-4.

Jasperson, Kory W., Thérèse M. Tuohy, Deborah W. Neklason, and Randall W. Burt. 2010. "Hereditary and Familial Colon Cancer." *Gastroenterology* 138 (6): 2044–58. doi:10.1053/j.gastro.2010.01.054.

Jiricny, Josef. 2006. "The Multifaceted Mismatch-Repair System." *Nature Reviews Molecular Cell Biology* 7 (5): 335–46. doi:10.1038/nrm1907.

Kinzler, Kenneth W., and Bert Vogelstein. 1996. "Lessons from Hereditary Colorectal Cancer." *Cell* 87 (2): 159–70.

López-Abente, Gonzalo, Javier García-Pérez, Pablo Fernández-Navarro, Elena Boldo, and Rebeca Ramis. 2012. "Colorectal Cancer Mortality and Industrial Pollution in Spain." *BMC Public Health* 12 (1): 589.

Mathews, Lesley A., Stephanie M. Cabarcas, and Elaine M. Hurt. 2012. "DNA Repair of Cancer Stem Cells." In *DNA Repair of Cancer Stem Cells*, 25–26. Dordrecht : Springer.

Midgley, R, and D Kerr. 1999. "Colorectal Cancer." *The Lancet* 353 (9150): 391–99.

Phillips, David H. 1999. "Polycyclic Aromatic Hydrocarbons in the Diet." *Genetic Toxicology and Environmental Mutagenesis*, Mutation Research, 443 (February): 139–47.

Rasmussen, Lene Juel, Christopher D. Heinen, Brigette Pokora-Royer, Mark Drost, Sean Tavtigian, Robert M.W. Hofstra, and Niels de Wind. 2012. "Pathological Assessment of Mismatch Repair Gene Variants in Lynch Syndrome: Past, Present, and Future." *Human Mutation* 33 (12): 1617–25.

Schütze, N. 2004. "siRNA Technology." *Molecular and Cellular Endocrinology* 213 (2): 115–19. doi:10.1016/j.mce.2003.10.078.

Shimada, Tsutomu. 2006. "Xenobiotic-Metabolizing Enzymes Involved in Activation and Detoxification of Carcinogenic Polycyclic Aromatic Hydrocarbons." *Drug Metabolism and Pharmacokinetics* 21 (4): 257–76.

Siegel, Rebecca, and Ahmedin Jemal. 2014. "Facts & Figures 2014-2016." http://yourhealthmatters.org/resources/Health%20Care%20Providers/ACS%20Colorectal%20Cancer%20Facts%26Figures%202014-2016.pdf.

Sinha, R. 2005. "Dietary Benzo[a]Pyrene Intake and Risk of Colorectal Adenoma." *Cancer Epidemiology Biomarkers & Prevention* 14 (8): 2030–34. doi:10.1158/1055-9965.EPI-04-0854.

Whitehead, Kathryn A., Robert Langer, and Daniel G. Anderson. 2009. "Knocking down Barriers: Advances in siRNA Delivery." *Nature Reviews Drug Discovery* 8 (2): 129–38. doi:10.1038/nrd2742.